Modeling and Optical Diagnostics of Iodine Fed Helicon Type Thrusters by a Detailed Global Model (DGM)

IEPC-2019-448

Presented at the 36th International Electric Propulsion Conference
University of Vienna • Vienna, Austria
September 15-20, 2019

Konstantinos Katsonis[1] and Chloe Berenguer[2]
DEDALOS Ltd., Thessaloniki, 54645, Greece

Daniele Pavarin[3], Fabio Trezzolani[4], Nicolas Bellomo[5], Marco Manente[6], Riccardo Mantellato[7], Davide Scalzi[8], Francesco Barato[9] and Alessandro Schiavon[10]
Technology for Propulsion and Innovation - T4i Ltd., Padova, Italy

Abstract: Iodine becomes a common electric thruster propellant due to its well known advantages. The iodine detailed global model developed by DEDALOS Ltd is used here for theoretical characterization and optimization of on ground prototypes, on the basis of plasma components composition diagrams and of functioning diagrams, giving a preview of the main species present in the thruster and of the electron density and temperature and allowing for the thruster functioning regimes analysis and optimization. Theoretical spectra, necessary for non-perturbing optical emission spectroscopy diagnostics are also obtained by the model. Experimental intensities of the spectral lines from an iodine-fueled RF electric thruster prototype, under development by T4i S.r.l., are compared with the corresponding theoretical ones from the model, leading to a detailed optical emission diagnostics.

Nomenclature

ξ_{TOT} = total ionization percentage
ξ'_{TOT} = electrons percentage
C-R = Collisional-Radiative
DGM = Detailed Global Model
DEDALOS = Data Evaluation and Diagnostics ALgorithms Of Systems Ltd.
ET = Electric Thruster
FD = Functioning Diagram

1 Director, katsonis.dedalos@gmail.com.
2 Project Manager, berenguer.dedalos@gmail.com.
3 CEO, d.pavarin@t4innovation.com.
4 Senior R&D engineer, f.trezzolani@t4innovation.com.
5 CTO, n.bellomo@t4innovation.com.
6 Plasma Propulsion Manager, m.manente@t4innovation.com.
7 Project Engineer, r.mantellato@t4innovation.com.
8 Project Engineer, d.scalzi@t4innovation.com.
9 Chemical Propulsion Manager, f.barato@t4innovation.com.
10 Technician, a.schiavon@t4innovation.com.

GM	=	Global Model
HelT	=	Helicon type ET
IDGM	=	Iodine Detailed Global Model
n_e	=	electron density
OES	=	Optical Emission Spectroscopy
p	=	pressure
P_{ABS}	=	absorbed power
PCC	=	Plasma Components Composition
Q_{TOT}	=	total flow rate
R	=	cone base radius
RF	=	Radio Frequency ET
T4i	=	Technology for Propulsion and Innovation S.r.l.
T_e	=	electron temperature
ThSpec	=	theoretical spectrum
H	=	cone Height

1. Introduction

IODINE has been often chosen nowadays as an Electric Thruster (ET) propellant, in view of its well known advantages[1]. The Iodine Detailed Global Model (IDGM)[2] developed by *DEDALOS Ltd* can provide theoretical characterization and optimization of on ground ET prototypes for this propellant, on the basis of Plasma Components Composition (PCC) diagrams and of Functioning Diagrams (FD). PCCs give a preview of the main species present in the ET and of the expected electron density n_e and temperature T_e values, while FDs allow for the thruster functioning regimes analysis and optimization. Moreover, theoretical spectra are obtained simultaneously by IDGM. These are necessary for non-perturbing Optical Emission Spectroscopy (OES) diagnostics of the thruster. Comparison of the spectral lines experimental intensities with the corresponding theoretical ones calculated by IDGM constitute the basis of OES.

Here we are interested in general in technology of the Helicon Thruster (HelT) type[3]. Helicon plasma thruster technology is developed in Padua by *T4i S.r.l.*, a spin-off of the University of Padua, in the frame of several international and Italian research projects[4]. In particular, in the experimental part contained in Section 4 we address specifically an example of iodine-fueled device belonging to the wider category of RF plasma thrusters, although largely based on Helicon technology. The considered prototype is a development model by *T4i S.r.l.* on the basis of the know how accumulated on Helicon[3,4] and more generally RF plasma sources[5]. By adapting IDGM input parameters to those prevailing in the RF thruster and after comparison of our theoretical results to experimental ones obtained recently by *T4i S.r.l.*, characterization and optical diagnostics of the prototype have been addressed.

IDGM encompasses detailed description of the neutral and of the singly and doubly ionized species present in the prototype. It also evaluates the absorbed power losses due to the main plasma processes which depend on the functioning conditions and gives mean values of the thruster plasma parameters.

Global Models (GM) of Iodine plasma have lately acquired a particular interest due to their application in characterization and in OES diagnostics of ETs of various types when fed by iodine[1,6], although using of iodine as ET propellant was suggested already at the beginning of the century[7]. The present work is based in a Detailed Global Model[8] (DGM) supported by an extended atomic database of iodine species, rather than using a Collisional-Radiative (C-R) iodine model, because the latter cannot take account of the sheath formation at the limits of the plasma and it is not addressing the energy losses detail. DGM allows for detailed characterization of ETs in an extended domain of absorbed power (P_{ABS}) values, provided the data of the expected ionized states are included in the system. This becomes more important when the ionization energy of the present species is low. For example, when P_{ABS} reaches values about 100 eV the twice ionized species have abundances similar to neutral ones for low pressures (see Section 2). Our IDGM calculations show that for P_{ABS} values of 1 keV, the presence of twice or more ionized iodine species becomes mandatory for low pressures. Presence of such species play a fundamental role in the thruster functioning and is essential for the thrust characterization. Study of the concomitant first and second order iodine spectra is necessary for any propulsion plasma OES diagnostics. Increase of the thruster energy class leads to considerable presence of more ionized iodine species, in particular when P_{ABS} per volume is higher. Calculation (and acquisition in case OES diagnostics is sought) of higher than the second order spectra should be addressed in this case.

In studying the iodine fed ETs, extensive use of Plasma Components Composition (PCC) diagrams and of Functioning Diagrams (FD) is made here, as was also the case e.g. in Ref. 1. Although low P_{ABS} values are of interest for the experimental application addressed here, we discuss PCCs belonging to P_{ABS} values going up to 100 W. Also, we comment a FD for iodine fed ETs for pressures going from 0.7 up to 5 mTorr, which for the low pressure region incorporates higher values of the total ionization percentage ξ_{TOT} , an often used parameter. Iodine propellant being unavailable *in situ* for interplanetary missions, it is important to insure its efficient use. In so doing, we also discuss the obtained total ionization during the thruster functioning, on the basis of two forms of FD giving the ξ_{TOT} dependence either on the pressure or on the absorbed power, two parameters which are very important for the thruster functioning.

Details of the elaboration of an averaged GM[9] and of the iodine homonuclear series structure are not described here, as both have been often made available in the literature. Iodine homonuclear series data resources and their evaluation have been discussed elsewhere (see Refs. 1,2 and references therein). In Section 2 we present modeling results pertaining to iodine fed thrusters obtained by IDGM, depending on the P_{ABS} , the pressure p and the electron temperature T_e . Section 3 is devoted to analyze the iodine fed ETs functioning on the basis of FD diagrams which also result from IDGM exploitation.

Following the review of the main IDGM results addressing the plasma composition and ionization, we compare obtained theoretical spectra with the corresponding experimental ones, which have been acquired by *T4i*. Iodine theoretical spectra given by IDGM are compared in Section 4 with the spectral acquisitions from MET to obtain OES diagnostics. We focus in the 470 nm to 575 nm spectral region, where important lines of both first and second order iodine spectra are present according to IDGM analysis. A preview of the expected thruster characteristics leading to its theoretical characterization are also addressed in this section. IDGM results are useful in controlling and diagnosing the plasma and contribute to optimize the thruster functioning. At the same time, OES diagnostics contributes to the model validation for low power class ETs, because theoretical spectra of neutral and singly ionized species from IDGM are here compared to experimental ones. Section 5 contains the obtained conclusions and the continuation sought for the present work.

2. Preview of plasma composition of iodine-fueled HelT following PCC diagrams

Plasma composition of iodine-fueled HelTs and RF thrusters in general for fixed flow rate values is investigated in this section, using PCC diagrams resulting from IDGM. For a given flow rate (Q_{TOT}) value, composition depends mainly on variation of two fundamental parameters, namely the absorbed power (P_{ABS}) and the pressure (p). Addressing a prototype of RF technology, a conical plasma form factor of R = 5 cm base radius and of H =15 cm height is selected. PCC diagrams illustrate the constitution of the plasma resulting after absorption of P_{ABS} , which is only a part of the available power and for given values of P_{ABS} and Q_{TOT} . Variation of the species populations is expressed as a function of p. Alternate presentations of the plasma constitution may also be obtained if p and one of the two other parameters Q_{TOT} or P_{ABS} are kept constant, while the other is varying. In general, Q_{TOT} , p, and P_{ABS} are subject to the conditions created *in situ*. The propellant feed can be conveniently regulated, while p and P_{ABS} depend on the thruster type, HelT, RF, etc. and rely mainly on the vacuum vessel or the space environment and the current produced by the solar cells or other available power devices.

First, results concerning low P_{ABS} values are addressed as we seek primarily application of our theoretical results to the *T4i* prototype case. However, IDGM encompasses detailed description of the HT also for high P_{ABS} values. We will tackle a case of 100 W P_{ABS} subsequently. In all, the P_{ABS} values addressed for the ET plasma having the aforementioned form factor vary from 25 W to 100 W. These values cover typical examples often considered in case of iodine-fueled ETs. The influence of the pressure and of the absorbed power on the ET plasma composition are separately addressed in this section, while the corresponding functioning of the thrusters will be discussed in Section 3. Note that in case of higher ET dimensions than those addressed here and for similar pressure values, the addressed values of the absorbed power have to be increased in a parametric way if the chosen feed amount remains the same, in case that sufficiently high ionization percentage is sought.

A. Plasma Composition as a Function of the Pressure *p*

We address low pressure values, varying from 0.8 mTorr to 5 mTorr while the iodine propellant feed remains at Q_{TOT} = 1 sccm. This feed is of interest to ETs of low power class. Composition of the plasma corresponding to the chosen feed and pressure region for an absorbed power of P_{ABS} = 25 W is shown schematically in Fig. 1. The presented results are obtained by the corresponding PCC.

The index 'TOT' used in Fig. 1 and similar ones, illustrating PCC results, indicate the total plasma density n_{TOT} (dot broken curve in magenta). For each of the various iodine neutral / ionized species a sum value including the densities of the totality of the corresponding Ground Level (GL) compound plus these of the corresponding excited ones is given. Results concerning the electron density n_e are given by a broken curve in red. In the case of Fig. 1 this curve is practically coinciding with the one giving the total population of the singly ionized species because of the quasi-neutrality principle in view of the very low values of the doubly ionized ones. Plasma component densities resulting from IDGM calculations are shown in general by curves in black for neutral species, in red for singly ionized and in blue for doubly ionized ones. Populations of the two GL components of the neutral iodine and of the five GL components of the singly ionized one are given separately, with the quantum core description in parenthesis. The small numbers attributed to the levels correspond to the order of each one in the corresponding Grotrian diagram.

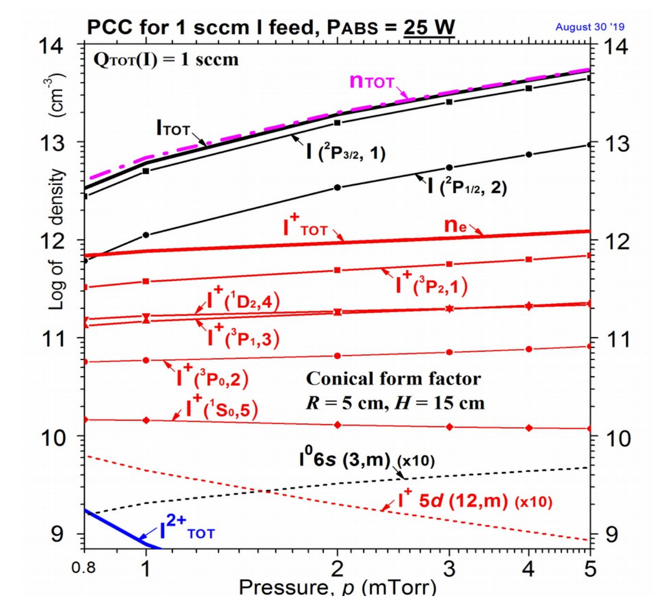

Figure 1. Pressure dependent PCC for P_{ABS} = 25 W and iodine feeding of 1 sccm

It can be seen in Fig. 1 that within the chosen p variation region the calculated species densities increase in general smoothly with pressure. A notable exception is the I^{2+} Ground Level (GL) sum, because the P_{ABS} value is very low given the chosen flow rate. Population of the total neutral iodine ground level I^0 GL remains similar to n_{TOT} for all the addressed pressure values. This reflects a rather low plasma ionization, especially for the higher pressures, with n_e going down to values of two orders of magnitude lower than n_{TOT} for pressure values of 5 mTorr.

As expected, populations of the excited states are clearly lower than the population of the corresponding GL compound. In order to include in Fig. 1 at least the more abundant excited species, their values have been multiplied by ten. Neutral 6*s* (n° 3) and singly ionized 5*d* (n° 12) species of metastable character denoted by "m" become then also visible. Note that populations of the latter is diminishing when p increase.

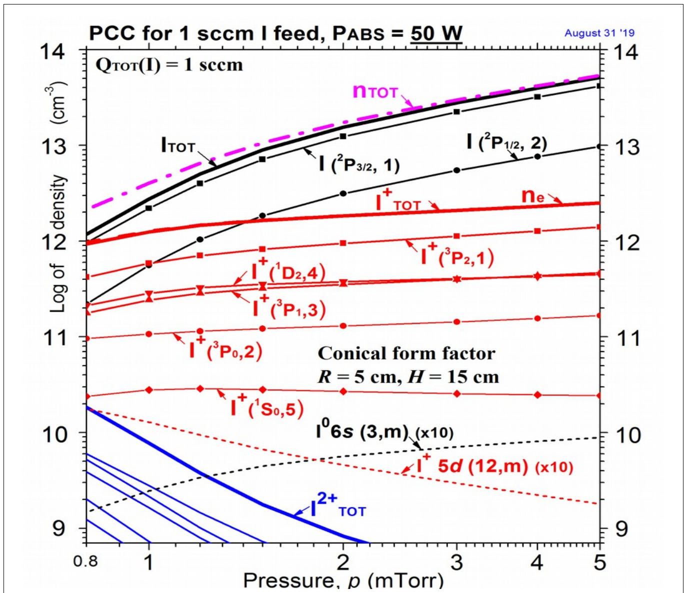

Figure 2. Pressure dependent PCC for P_{ABS} = 50 W and iodine feeding of 1 sccm

A situation similar to this of Fig. 1, except in what concerns the absorbed power, which is doubled to P_{ABS} = 50 W is given in Fig. 2. In this case the plasma is obviously more ionized and consequently the values of the total density of the twice ionized iodine I^{2+}_{TOT} shown in the low p region are higher, with its partial GL populations also visible.

Complementary information on the characteristics of the two plasma cases illustrated by Figs. 1 & 2 is provided by Figs. 3 & 4 which are concomitant to Figs. 1 & 2 correspondingly. Colors attributed to the iodine species in the figures are similar to those used previously. Figs. 3 & 4 address more specifically percentages of the main plasma ionized constituents. Corresponding electron temperatures T_e are also indicated by red thin curves bearing full squares ■. Evaluation of T_e is mandatory for ET characterization and diagnostics. Total ionization percentage ξ_{TOT} = n_{ION} / n_{TOT} and electrons percentage ξ'_{TOT} = n_e / n_{TOT} are also shown by black lines, continuous with full dots and broken with empty dots correspondingly. As was often the case, the parameter ξ_{TOT} used here as a measure of the plasma ionization, addresses only the sum of each ion type numbers, irrespectively of the ionization charges. Then, in calculating the resulting thrust, the number of each ion must be multiplied by the number of the charges that each ion bears in order to arrive to a value equal to ξ'_{TOT} = n_e / n_{TOT} in conformity with the quasi-neutrality assumption. Consequently, ξ'_{TOT} may exceed 100 % , at least for low pressures where the ionization is considerable and leads to sustainable presence of at least twice ionized iodine species densities.

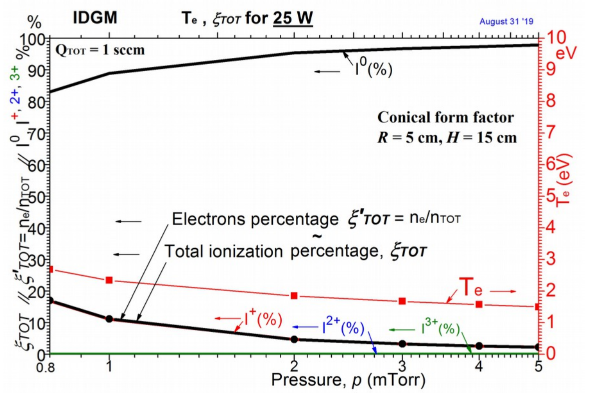

Figure 3. PCC conjugate for P_{ABS} = 25 W

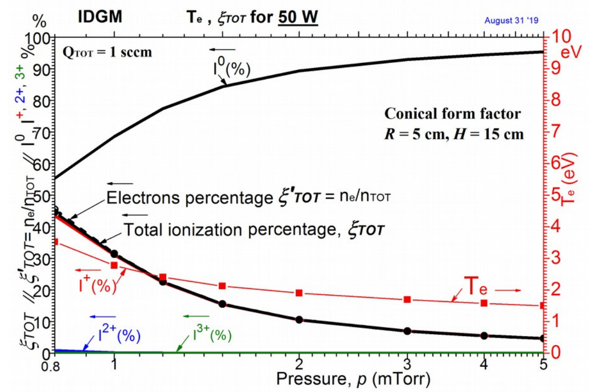

Figure 4. PCC conjugate for P_{ABS} = 50 W

Fig. 3 concerning an absorbed power value of P_{ABS} = 25 W shows that ξ'_{TOT} has practically similar values with ξ_{TOT} as expected in case of very low double ionization. These values could easily approach 20 % for low pressures, where the ionization is considerable, while when p increases become negligible. T_e increases slowly when the pressure is diminishing down to 0.8 mTorr. Fig. 4 pertain to an absorbed power of P_{ABS} = 50 W. It shows that values of ξ'_{TOT} become slightly different than those of ξ_{TOT} for low pressures, where the ionization is increasing, with presence of twice ionized iodine species densities. T_e increases fast for pressure values around 0.8 mTorr.

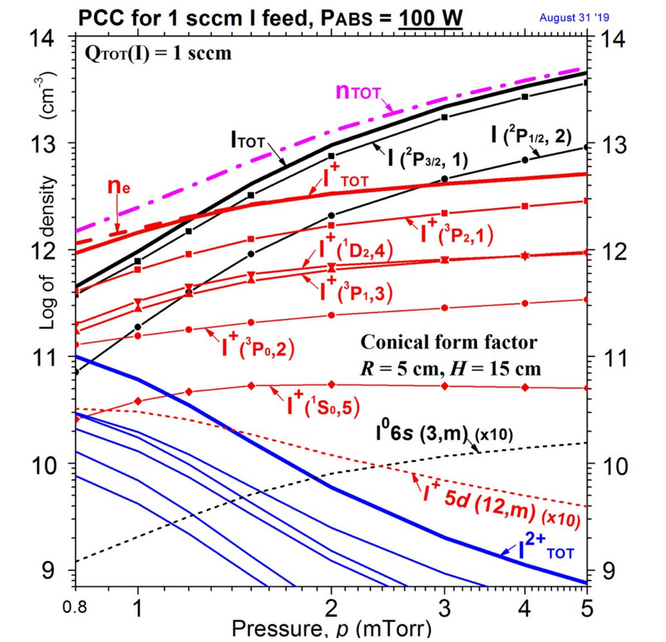

Figure 5. Pressure dependent PCC for P_{ABS} = 100 W and iodine feeding of 1 sccm

For increased P_{ABS} values even higher ionization values are reached. Situation pertaining to absorbed power of 100 W is illustrated in Fig. 5, with a PCC showing high ionization for low pressures, although persistent increase of the neutral species presence in case of high pressures is manifested.

Percentage of the singly ionized species is increasing up to pressures of about 2 mTorr, reaching a plateau for higher pressure values. In the high pressure region, presence of all the ionized species with q > 1 is low and I^+ follows practically the total ionization percentage values.

Interestingly, contribution of twice ionized species to positive charges arrives up to 2x10^{11} cm^{-3} for 0.8 mTorr, although their number is five times lower than this of the neutral iodine species, as it can be seen in Fig. 5. Then, an increase of the P_{ABS} values to 100 W allows for a quite improved utilization of the propellant in case the pressure stays at the level of a few mTorr, thus allowing for convenient thrust values.

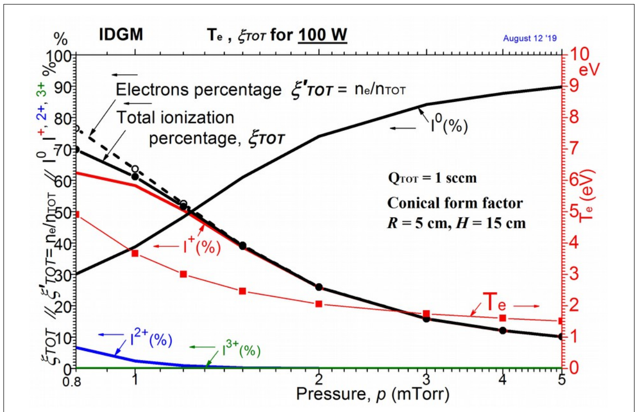

Figure 6. PCC conjugate for P_{ABS} = 100 W

We described here ET plasma composition by a PCC for the typical case of 100 W absorbed power. In order to obtain a better insight of the situation, we may address a conjugate diagram, similar to these shown in Figs. 3 & 4. This diagram is contained in Fig. 6. In this figure, it can be observed that the electron temperature varies from 1.5 eV to 5 eV approximately, while the pressure diminishes from 5 mTorr to 0.8 mTorr. Inversely, when pressure increases from 0.8 mTorr to 5 mTorr, the percentage of neutral iodine increases drastically from 30 % up to 90 %. It has also to be noticed that because of the sufficient absorbed power value of 100 W, twice ionized iodine species are visible for low pressure values and have about 7 % presence for 0.8 mTorr. Consequently, as shown in Fig. 6, ξ'_{TOT} has a higher value than the ξ_{TOT} one in the low pressure region, where the ionization is considerable with sustainable presence of twice ionized iodine species densities.

B. Influence of the absorbed power P_{ABS} on the plasma composition illustrated by an 1 mTorr modified PCC

The mandatory role which the absorbed power plays on the plasma equilibrium conditions of ET functioning can be appreciated through Fig. 7, presenting a power depending PCC diagram which gives the plasma composition for the same form factor as before in case of an indicative pressure of 1 mTorr, with the feed set always at 1 sccm. P_{ABS} varies from 25 W to 100 W. Symbols and colors in Fig. 7 are the same with those of Figs. 1 to 6. As the pressure must stay constant at 1 mTorr, n_{TOT} diminishes slowly with absorbed power in Fig. 7, divided by about three when P_{ABS} is increasing four times. As was illustrated in Figs. 1 & 2, the bulk of the plasma ionization for about 1 mTorr pressure is following the curve giving the density of the singly ionized species, with values of n_e and of I^+ GL compound being about the same and only for high absorbed power appears a small difference. Both n_e and I^+ GL increase slowly to approach the n_{TOT} values with increasing P_{ABS} . It is to be noted that, beginning with about P_{ABS} = 80 W, the I^{1+} GL compound species become more abundant than the neutral ones. The fact that for higher P_{ABS} values the difference between n_e and I^+_{TOT} becomes distinguishable was already observed in Fig. 6. For 1 mTorr, trebly ionized I^{3+} species are so scarce that are not included in Fig. 7.

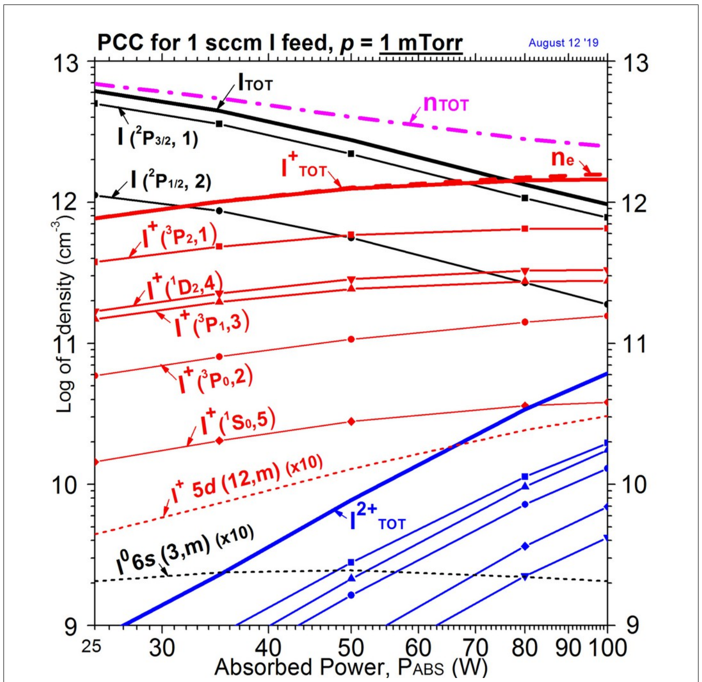

Figure 7. Power dependent PCC for p = 1 mTorr and iodine feeding of 1 sccm

Populations belonging to the various cores of the neutral and of the ionized species are shown separately by thin curves of various types, marked in parenthesis by 1 to 5 following the atomic descriptions except for twice ionized species. Expressing the plasma density as a function of the absorbed power gives an interesting insight of the plasma behavior.

A diagram concomitant to the PCC shown in Fig. 7, is contained in Fig. 8 and gives additional aspects of the plasma properties under the same conditions prevailing for Fig. 7. Fig. 8 is somewhat similar to Figs. 3, 4 & 6 and uses the same symbols. However, species percentages and T_e values are given here as a function of the absorbed power, instead of using the pressure as ordinate and results are concomitant to those presented in Fig. 7.

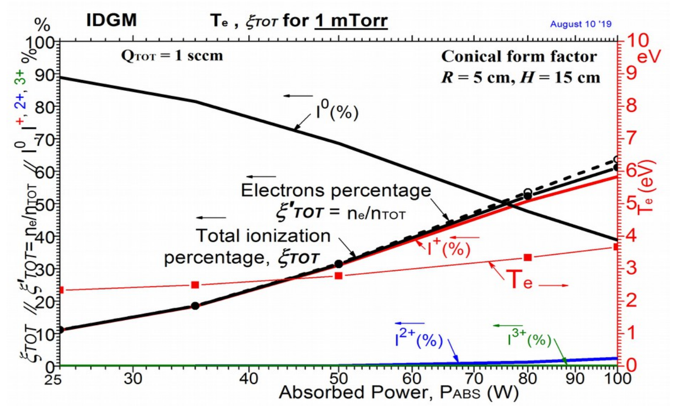

Figure 8. Power dependent PCC conjugate for $p = 1$ mTorr

It is to be noticed that for about P_{ABS} = 75 W neutral and singly ionized species have similar values, e.g. 50 % of the provided propellant is practically not used for thrust. Doubly ionized species contribute very little to the total plasma ionization even for high P_{ABS} values and appear at the bottom of the figure, with trebly ionized species practically absent.

As reported previously, ξ_{TOT} and ξ'_{TOT} percentages, shown by continuous and dashed black curves correspondingly, are very similar for high P_{ABS} values but have quite distinguishable values when absorbed power values exceed, say, P_{ABS} = 50 W.

3. Characterization and optimization of iodine-fueled HelTs using FD diagrams

A detailed description of the expected functioning of a prototype thruster and its theoretical characterization can be obtained by using of a dedicated FD. Typically, FDs provide the propellant ionization percentage as a function of the pressure. They contain parametric curves for various values belonging to concomitant electron temperature and P_{ABS} values. Thus, a FD provides in condensed form a set of PCCs. Alternatively, FDs illustrating the propellant ionization according to the variation of P_{ABS} or of Q_{TOT} can be obtained. The IDGM model has been used to obtain both the FD diagram types presented in this section, belonging to an iodine-fueled thruster with the form factor addressed previously in Section 2.

In Part A we show how a FD can be used in order to obtain a detailed insight on the thruster functioning. Optimal functioning conditions of iodine-fueled HelTs are also investigated by a modified FD diagram giving ionization vs absorbed power. Such a FD will be shown in Part B.

A. Preview of iodine-fueled HelT devices characteristics by ionization vs pressure FD diagrams

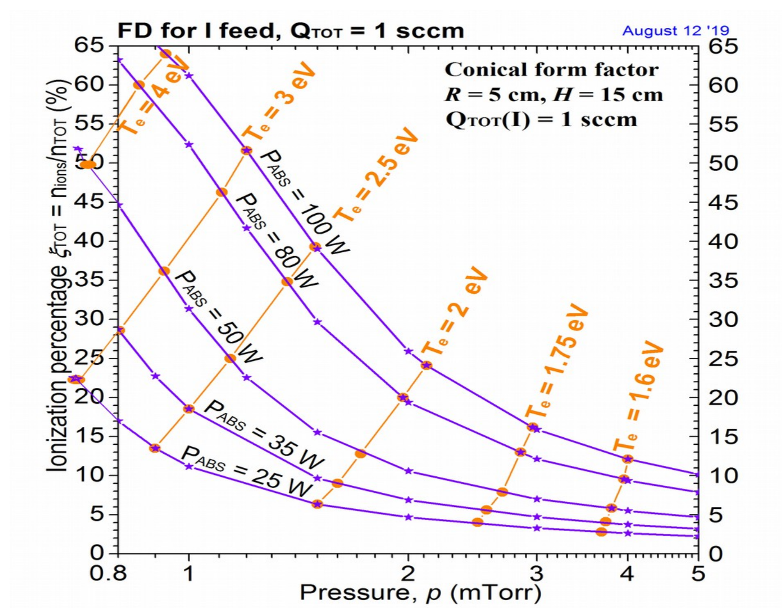

Figure 9. FD for Q_{TOT}(I) = 1 sccm and pressure range from 0.8 mTorr up to 5 mTorr

A typical FD is shown in Fig. 9, in which the ionization percentage ξ_{TOT} is given for pressure values varying from 0.8 mTorr to 5 mTorr. This figure contains iso-power curves for P_{ABS} values varying from 25 W to 100 W and iso-thermic curves for T_e values varying from 1.6 eV to 4 eV. As expected, curves of this figure illustrating ξ_{TOT} values vary considerably as a function of the pressure in the region of low pressure values, while when the pressure is quite high ξ_{TOT} remains low even for high P_{ABS} values. Hence, functioning of the thruster under conditions corresponding to the right region of Fig. 9 is not to be considered because even with high absorbed power values big part of the propellant quits the thruster without contributing to the thrust. The temperatures corresponding to the given iso-thermic curves increase faster for lower pressures because ξ_{TOT}

is quite high there. With diminishing *p,* iso-power curves approach to draw lines for lower power values, corresponding to faster ξ_{TOT} increase. This indicates that the pressure diminishing is more efficient in the low pressures region.

B. Optimal functioning conditions of iodine-fueled HelTs by ionization vs absorbed power FD diagrams

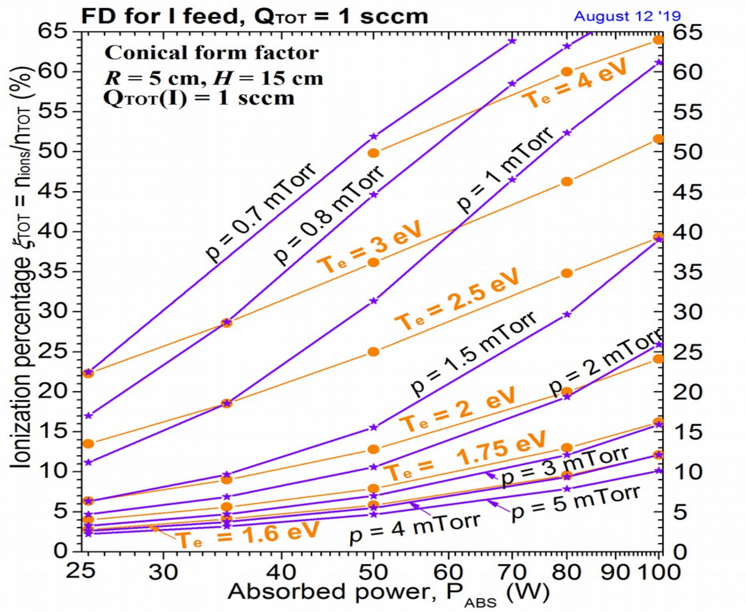

Figure 10 : Modified FD for Q_{TOT}(I) = 1 sccm and P_{ABS} from 25 W to 100 W.

Using of an alternate form of FD diagrams can address the optimizing of an iodine-fueled thruster. This is illustrated in Fig. 10, addressing variations of T_e and of P_{ABS} values in the same intervals with those of Fig. 7, but with ionization variations given as a function of the P_{ABS} instead of the pressure. A feed of 1 mTorr is considered throughout.

Pressure values (of 0.7 mTorr, 0.8 mTorr, 1.0 mTorr, 1.5 mTorr, 2.0 mTorr, 3.0 mTorr and 5.0 mTorr), given in Fig. 10 by starred curves follow loosely the temperature ones, but higher pressures belong to lower temperatures. A novel view of a thruster functioning is given by Fig. 10, illustrating the obligation for the pressure values to stay small if we want to obtain sufficient ionization of the provided propellant without increasing excessively the absorbed power amount.

4. Analysis of iodine experimental and theoretical spectra aiming OES diagnostics

It is well known that the DGMs allow also for theoretical evaluation of the spectral line intensities, which by comparison with the experimental ones give the ne and Te values of the thruster plasma. Argon theoretical plasma spectral lines, obtained by Collisional-Radiative or Global models have been used previously in OES diagnostics[10,11]. In the same direction, analysis of theoretical xenon spectra has been made, leading to interesting results[12]. Because of the similarities between Xe and I atoms, we expect results which eventually should be compared advantageously, even if their chemical properties are clearly different. Aiming OES diagnostics of the aforementioned iodine-fueled prototype developed in Padua, we focused on plasma conditions expected to prevail during its functioning. The employed thruster has an envelope contained in a ϕ 55 x l 120 mm cylinder, weights approximately 0.4 kg and is characterized by a very simple structure, including a ceramic discharge chamber, an RF antenna for plasma ionization and a magnetic system based on SmCo permanent magnets, all housed within a metallic structure.

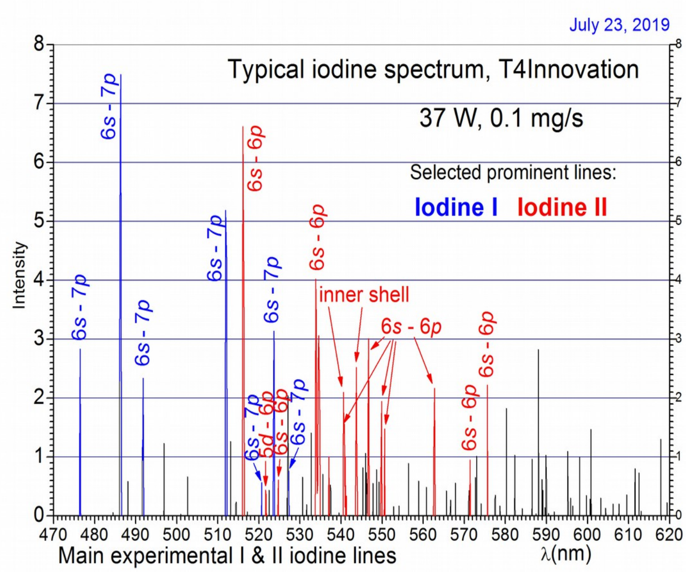

Figure 11. Part of the experimental iodine I & II spectrum

Acquisition of the plasma experimental spectra, together with the PCC and the FD diagrams and theoretical spectra which are obtained from IDGM, contribute efficiently to theoretical characterization and to OES diagnostics. This has been demonstrated previously for other electric thruster types fed by iodine[1]. In Fig. 11 we address a typical spectrum acquired recently by *T4i* from the thruster plasma, in the spectral region which is contained between 470 nm and 620 nm shown.

Measured intensities are given in Fig. 11 with the prevailing conditions also reported. In particular, the spectra were observed in the thruster plasma, placing an optical fiber approximately 5 mm downstream its exhaust section, oriented orthogonally to the axis of the thruster. The plasma has roughly a conical form and expands rapidly downstream the thruster, thus making it difficult to precisely estimate the actual pressure and size of the discharge in the region of interest, although an approximated estimation can be performed.

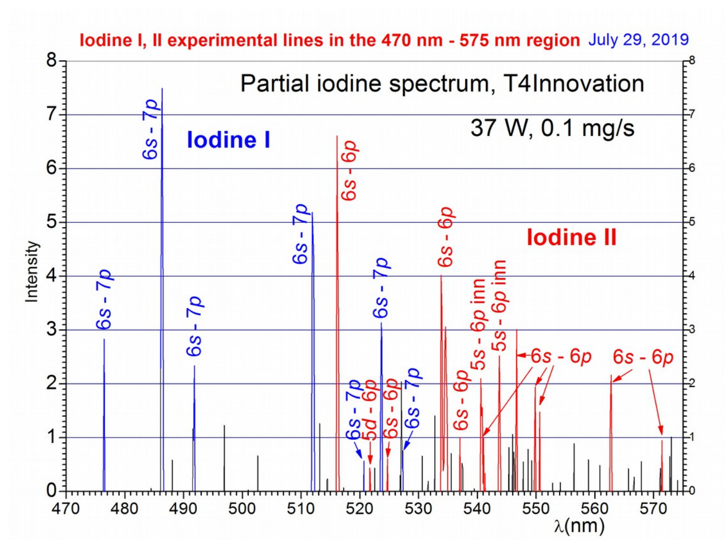

Figure 12. Experimental iodine I & II spectrum in the 470 nm to 575 nm region

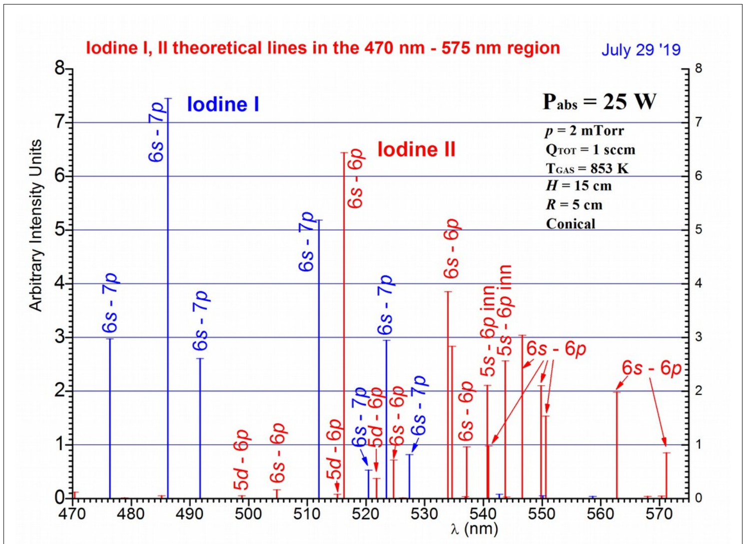

Figure 13. Iodine I & II spectrum in the 470 nm to 575 nm region, obtained by IDGM

Iodine I & II transitions are contained, with some prominent neutral lines in blue and ionic ones in red, following analysis by IDGM. Overall comparison of I I with I II intensities indicates a substantial ionization. Rates of experimental vs theoretical lines intensities allow for OES. Experimental spectra as this of Fig. 11, together with the PCC and the FD diagrams obtained from IDGM contribute efficiently to theoretical characterization and to diagnostics of iodine fed HelTs. This has been demonstrated previously for other electric thruster types[3] fed by iodine.

Part of the provided experimentally acquired spectrum contained in Fig. 11 is reported in Fig. 12, in which we noted also prominent spectral lines of the first and the second iodine spectrum by blue and red lines respectively. Lines belonging to the 6*s* – 7*p* multiplet of the neutral iodine and to the 6*s* – 6*p* multiplet of singly ionized iodine are shown, together with two inner-shell lines of the latter. In Fig. 13 we focus in the 470 nm to 575 nm spectral region containing important lines of both the neutral and the ionized iodine spectra in order to optimize the OES diagnostics. Information about the plasma dimensions, the pressure and the iodine flow rate is also provided in Fig. 13. After searching among the set of our theoretical spectra in the same region, we identified the theoretical spectrum shown in Fig. 13 as corresponding to the experimental. In this figure theoretical I I & II lines are shown for iodine feed of Q_{TOT} = 1 sccm. Pressure is of 2.0 mTorr and P_{ABS} of 25 W.

Comparing Fig. 13 with Fig. 12, it is seen that for both the I^0 and I^{+1} species the intensities of the theoretical lines are analogous to the experimental ones given in Fig. 12. Also the ratio of the neutral lines intensities versus the ionic ones is similar in the experiment and in the theory. As the 1 sccm feed is about 0.1 mg/s in case of Xe or I feed, we infer that the absorbed power is 25 W for a pressure of 2 mTorr. Following Fig. 3 of Section 2, the approximate electron temperature is 1.8 eV with an ionization percentage of 5 % for an approximate pressure value of 2 mTorr. Because in the addressed region the theoretical spectrum shown in Fig. 13 is very similar to the experimental one of Fig. 12, we conclude that the experimental conditions are comparable with the ones corresponding to the spectral calculations. The global comparison of the theoretical spectra multiplets with the experimental ones illustrated here, minimize errors coming from the atomic data and gives also an evaluation of the ionization percentage.

In order to check the model output, another estimate of the ionization percentage was performed by *T4i* by estimating the total ion current ejected by the thruster using a Faraday probe, which gave substantially higher values, in the range of 50-85%. Such wide uncertainty margin accounts for several factors hampering the accuracy of Faraday probe measurements, such as ion focusing and secondary electron emission, which typically lead to an over-estimation of the measured current. Other minor effects usually come from geometrical uncertainties in the set-up.

Even considering all this, however, Faraday probe estimations exceed spectroscopic ones by a considerable margin; this may be due to a number of reasons, among which the most probable are

i) uncertainty in the estimation of the plasma discharge characteristics (pressure, size) in the section of interest,

ii) inhomogeneities in plasma distribution within the plume, leading to zones of locally low density and

iii) the relatively small wavelength span employed in the first spectroscopic acquisitions. Plume inhomogeneity, in particular, is likely the main source of disagreement, since the spectroscopic measurements considered in this work are related to a relatively small, fixed spot in the plume, while Faraday probe measurements involved radial scans of the plume for ion current integration and are thus of a global nature.

Further testing is required in order to rule out these and possibly other elements, in order to achieve a reasonable agreement between Faraday probe and spectroscopic measurements which, in our opinion, is required for a sound testing procedure. More detailed comparisons aiming to conclude with the RF plasma thruster characterization and diagnostics, based to additional experimental spectra, is in progress.

5. Conclusions and perspectives

We conclude that the PCC and the FD diagrams together with the theoretical spectra obtained from IDGM contribute efficiently in characterizing theoretically iodine-fueled HelT and more generally RF plasma thrusters and allow for a support for their OES diagnostics. Moreover, as was also the case previously with other thruster types fed by iodine, experimental support by acquisition of experimental spectra corresponding to theoretical ones gives the possibility to obtain OES diagnostics of the thruster plasma. It also corroborates the theoretical results already obtained by the IDGM model on the basis of the experimental results.

In particular, *T4i* is willing to continue the spectroscopic analysis on its RF thrusters and will likely extended it in the future to the REGULUS propulsion system, currently under development and based on an iodine-fed RF thruster[5,13,14]. The new tests will include spectral acquisitions with a wider wavelength span, in order to provide more data to tune the model, as well as spectroscopic measurements at multiple radial locations in the plume.

References

[1]Berenguer, Ch., Katsonis, K., and Gonzalez del Amo, J., "Using of an Iodine Detailed Global Model for Characterization and for Optical Diagnostics of Helicon Thrusters," *6th Space Propulsion Conference*, Paper ID SP2018_**215**, Seville, Spain, May 2018

[2]Katsonis, K., and Berenguer, Ch., "A Detailed Global Model of Iodine Plasma for Optimization and Diagnostics of Electric Thrusters," *Imperial Journal of Interdisciplinary Research*, vol. **2**, Issue 12, 166, p. 1093, November 2016

[3]Pavarin, D., Ferri, F., Manente, M., Lucca Fabris, A., Trezzolani, F., Faenza, M., Tasinato, L., Tudisco, O., De Angelis, R., Loyan, A., Protsan, Y., Tsaglov A., Selmo, A., Katsonis, K., Berenguer, Ch., Packan, D., Jarrige, J., Blanchard, C., Elias P. Q., and Bonnet, J., "Thruster Development Set-up for the Helicon Plasma Hydrazine Combined Micro Research Project (HPH.com)," *32nd International Electric Propulsion Conference*, IEPC-2011-**241**, Wiesbaden, Germany, September 2011

[4]Pavarin, D., Lucca Fabris, A., Trezzolani, F., Manente, M., Faenza, M., Ferri, F., Selmo, A., Katsonis, K., and Berenguer, Ch. "Low Power RF Plasma Thruster Experimental Characterization", *48th AIAA Conference*, AIAA 2012-**4191**, Atlanta, GE, USA, July-August 2012

[5]Manente, M., Trezzolani, F., Magarotto, M., Fantino, E., Selmo, A., Bellomo, N., Toson, E., and Pavarin, D., "REGULUS: A Propulsion Platform to Boost Small Satellite Missions," *Acta Astronautica*, vol. **157**, 241-249, 2019

[6]Katsonis, K., Berenguer, Ch., Scharmann, S., Gärtner, W., Holste, K., Köhler, P., Mitić, S. and Klar, P.J., "Global Model Based Development of Electric Thrusters Using Iodine Propellant," *5th Space Propulsion Conference*, Paper ID SP2016_**3125322**, Rome, Italy, May 2016

[7]Dressler, R. A., Chiu, Y.-H., and Levandier, D. J., "Propellant Alternatives for Ion and Hall Effect Thrusters," *38th Aerospace Sciences Meeting and Exhibit*, AIAA-2000-**0602**, Reno, NV: American Institute of Aeronautics and Astronautics, January 2000

[8]Katsonis, K., and Berenguer, Ch., "Using of Detailed Global Models," update of *ResearchGate project : ISRU Based Electric Propulsion*, December 2016

[9]Katsonis, K., and Berenguer, Ch., "Global Modeling of N_2O, Air and N_2 Discharges and Applications," *Lambert Academic Publishing*, Saarbrucken, Germany, October 2013

[10]Katsonis, K., Berenguer, Ch., Pavarin, D., Lucca Fabris, A., Trezzolani, F., Faenza, M., Tsekeris, P., Cohen, S., and Cornille, M., "Optical Diagnostics of a Low Temperature Argon Thruster," *32nd International Electric Propulsion Conference*, IEPC-2011-**169**, Wiesbaden, Germany, September 2011

[11]Berenguer, Ch., and Katsonis, K., "Plasma Reactors and Plasma Thrusters Modeling by Ar Complete Global Models," *International Journal of Aerospace Engineering*, vol. **2012**, Article ID 740869, September 2012

[12]Katsonis, K., Berenguer, Ch., Pavarin, D., Trezzolani, F., Manente, M., and Gonzalez del Amo, J., "A Xenon Detailed Global Model in Support of Electric Propulsion Technology," *6th Space Propulsion Conference*, Paper ID SP2018_**212**, Seville, Spain, May 2018

[13]Bellomo, N., Roberto, R. D., Toson, E., Pavarin, D., and Graziani, F., "REGULUS Electric Propulsion Module IoD in UniSat-7 Mission," *SmallSat, AIAA 33rd Annual Conference on Small Satellites,* Utah Sate University, Logan, UA, USA, 3-8 August 2019

[14]Manente, M., Bellomo, N., Toson, E., Trezzolani, F., Mantellato, R., Cappellini, L., Scalzi, D., Minute, M., Schiavon, A., Magarotto, M., and Pavarin, D., "REGULUS: Iodine Fed Plasma Propulsion System for Small Satellites," IEPC-2019-**417**, this Conference